

## Design and Status of Solar Vector Magnetograph (SVM-I) at Udaipur Solar Observatory

Sanjay Gosain<sup>1,2,\*</sup>, P. Venkatakrisnan<sup>1</sup> & K. Venugopalan<sup>2</sup>

<sup>1</sup>*Udaipur Solar Observatory, P. O. Box 198, Dewali, Bari Road, Udaipur 313 001, India.*

<sup>2</sup>*Mohanlal Sukhadia University, Udaipur 313 001, India.*

\**e-mail: sgosain@prl.res.in*

**Abstract.** We present the status of the instrument called Solar Vector Magnetograph Phase-I (SVM-I) currently being developed at Udaipur Solar Observatory. SVM-I is an instrument which aims to determine the magnetic field vector in the solar atmosphere by measuring Zeeman induced polarization across the spectral line. The instrument is currently in a preliminary development stage, with all components under an evaluation process. The integration of components is being done. The integrated performance of the system on a tracking mount and its control software is being tested. Some test observations of sunspots has been carried out. In this paper we give a technical description of the hardware and software elements of the instrument and present the polarized images obtained during test observations.

*Key words.* Sun: polarimetry—Fabry–Perot—solar magnetic fields.

### 1. Introduction

It is widely accepted that the source of explosive phenomena on the Sun is the interplay between magnetic fields and solar plasma. The measurement of vector magnetic fields is of great importance in order to develop a better understanding of these explosive phenomena and to be able to predict these events. The spectral lines from regions permeated by magnetic fields are Zeeman split. In visible wavelengths, the Zeeman splitting is measurable only for strong field regions like in sunspot umbrae, while, in the infra-red wavelengths one is able to observe splittings for most of the active region field strengths. However, even when the splitting is not resolved, the polarization of the Zeeman components provides a diagnostic tool for inferring the magnetic field vector. Thus, the problem of quantifying the magnetic field reduces to measurement of the full polarization state of the Zeeman components, which is represented in terms of Stokes vector.

Conventionally, the polarimetry techniques employ wave retarders for modulation like crystal waveplates, electro-optic crystals like KDP or nematic and ferro-electric liquid crystals or Photo Elastic Modulators (PEMs) with polaroids or calcites as the analyzers. For spectral isolation one uses either dispersive methods like grating spectrograph or interferometric methods like Michelson cubes or Fabry–Perot interferometers or bi-refringent filters.

In this paper we describe the design and status of Solar Vector Magnetograph Phase-I (SVM-I). The paper is organized as follows. The optical design and a brief layout of various components of the instrument is described in section 1. In section 2, we describe the characteristics of various subsystems of the magnetograph. Section 3 describes the control software used for acquiring data and controlling the instrument. In the last section, the first-light images of a sunspot and very preliminary analysis is presented. The evaluation of the data is under progress, which will eventually drive the design modifications in second phase of solar vector magnetograph.

## 2. Schematic description of the instrument

### 2.1 Imaging system

Figure 1 shows the schematic layout of the instrument. The primary imaging is done using a Schmidt–Cassegrain telescope of 20 cm aperture. A broadband interference filter of bandpass 15 nm is placed in front of the telescope to prevent excessive heating of the telescope optics. The bandpass is centered around 630 nm to allow the Fe I line pair in which we are interested to do polarimetry. The focal length of the telescope is 2 metres, this makes an  $f/10$  beam. The image of the Sun is formed on a field stop where a circular aperture selects a desired field-of-view on the Sun.

### 2.2 Polarimeter

The light passing through the aperture is analyzed for polarization using the polarimeter module which consists of two quarter wave-plates mounted on a high resolution rotary stage. These wave-plates, which are compound zero-order quartz wave-plates, are used

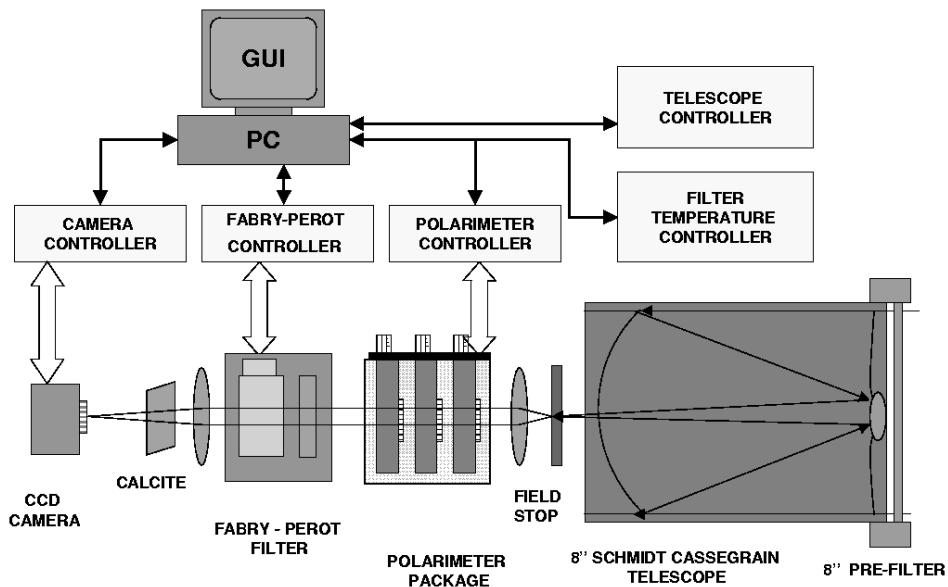


**Figure 1.** A schematic layout representing the optical and controls layout of the Solar Vector Magnetograph.

**Table 1.** Wave-plate orientations for the polarimeter.

Stokes parameter	Wave plate 1	Wave plate 2
$I \pm Q$	$0^\circ$	$0^\circ$
$I \mp Q$	$45^\circ$	$45^\circ$
$I \pm U$	$0^\circ$	$45^\circ$
$I \mp U$	$0^\circ$	$135^\circ$
$I \pm V$	$45^\circ$	$0^\circ$
$I \mp V$	$135^\circ$	$0^\circ$

to modulate the polarized light signals. The retardation properties of these wave-plates were tested in a laboratory using a technique which employs Babinet compensator and CCD camera, as described in Sankarasubramanian & Venkatakrishnan (1998). The orientation of the wave-plates are adjusted through computer control to filter out desired Stokes parameters. The orientations of the two wave-plates for different Stokes measurement are given in Table 1. A total of three measurement positions are required to measure the complete Stokes vector. Since, the polarimetry is done in diverging beam and retardation of wave-plates vary with angle-of-incidence, this has two effects. Firstly, the retardation varies across the field-of-view (FOV), which is negligible as our FOV is only few arc-minutes. Secondly, the value of retardation has a spread around a mean value. The amount of spread depends on half of the cone-angle of the diverging beam. In our case for  $f/10$  beam the half cone-angle is  $2.8^\circ$ , which corresponds to a variation of retardation of around  $1.5^\circ$  from true retardation value, which is not significant considering the errors of retardation across the area of retarder and misalignment errors in polarimeters. In the present design the retarders are not kept in collimated beam because there will be a systematic variation of retardance across the field-of-view and also the reflections from the back surface of wave-plates produces problematic ghost images. The analysis of polarization is done using two crossed-calcite polarization analyzer assembly placed just before the CCD camera.

### 2.3 Fabry–Perot filter & CCD camera

After the polarization modulation by the wave-plates, the beam is collimated using a lens of focal length  $f = 180$  mm. This amplifies the angles of the incoming light by about a factor of 11. The collimated beam passes through Fabry–Perot (FP) etalon. The etalon is an air spaced peizo-scanned and servo controlled etalon (Hicks *et al.* 1984). The FWHM of the transmission band of FP is determined to be about  $120 \text{ m\AA}$  using laser in laboratory (Choudhary & Gosain 2002) and also using telluric lines formed in Earth’s atmosphere. The collimated design suffers from the problem of spectral shift across the field-of-view but offers better spectral resolution than telecentric design and is more compact. The scanning FP etalon can be calibrated for FOV shift as full line profiles are available. The adjacent transmission peaks of the FP are blocked using a narrow-band interference filter. This filter is a two-cavity filter with a pass-band of  $0.35 \text{ nm}$ . The filter is kept in a temperature controlled oven with temperature stability of  $\pm 0.5^\circ\text{C}$ . The beam is finally re-imaged using a lens of  $f = 500$  mm which gives a magnification of 2.7 times. The final image scale is around  $0.87 \text{ arcsec}$  per pixel. The converging beam is passed through a calcite polarization analyzer assembly placed

just before the CCD camera. This makes two identical images of the region in orthogonally polarized light. The two images are simultaneous and hence immune to seeing induced spurious polarization signals. The CCD camera is Apogee AP6E camera, which uses a KAF 1001E image sensor consisting of  $1024 \times 1024$  pixel array with square pixel of size  $24 \mu\text{m}$ . The pixels are digitized up to 14 bits at a speed of 1 MHz. Typical readout time for full frame, without binning, is about 1.3 seconds.

#### 2.4 Tracking system and housing

The entire assembly of SVM optics is straight and symmetric about the optic axis with no oblique reflections. Thus, the instrumental polarization is expected to be minimal. The stress induced polarization in the broad-band eight inch pre-filter is yet to be determined, but is expected to be negligible as was the case in the MSFC magnetograph (Hagyard *et al.* 1982). The length of the SVM optical setup is about 1.6 meters in length. The individual modules are fixed on to movable base plates, which are then fixed on optical rail at the desired locations. The entire rail is mounted on German Equatorial mount. Presently the mount works without solar guider, but the polar alignment is accurate enough to track a sunspot within a few arc-seconds for a time duration of 5 to 6 minutes. This duration is long compared to the time required to make one complete Stokes measurement. The entire system is housed on the roof-top of USO main campus, a temporary platform with a sliding dome is developed to house the instrument (see Fig. 2).



**Figure 2.** A view of the SVM Phase-I test set-up on the terrace of USO, Udaipur main campus building. The sliding dome is pushed backwards here and the SVM optics mounted on German Equatorial mount.

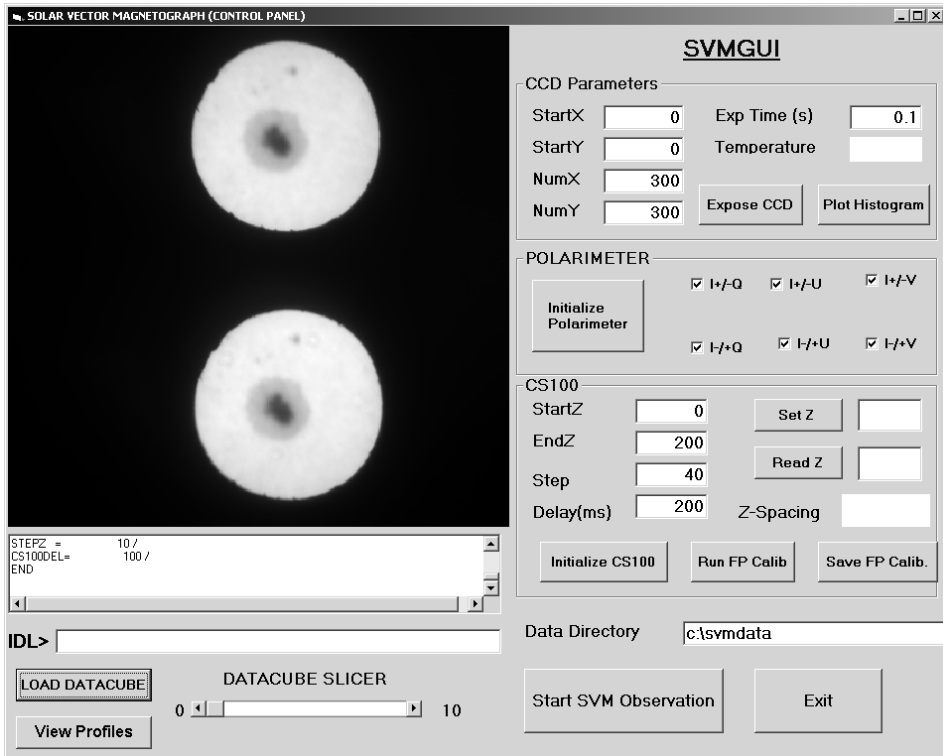


**Figure 3.** A snapshot of GUI for data acquisition and control of SVM instrument. The quicklook analysis of raw data can be done using IDL activeX on this interface.

### 2.5 Control software

The control software for the instrument has been developed in-house using Visual Basic on Microsoft Windows platform. The concept behind the software development has been to use ready-made software components like ActiveX drivers, COM modules, Dynamic Linked Libraries (DLLs), etc. from instrument vendors or third parties and integrate them together to be controlled under a single application. The CCD camera is controlled using ActiveX drivers supplied by the manufacturer. Similarly, the polarimeter rotary stages are controlled using COM modules from GPIB card vendor. The RS232 commands are sent using MSCOMM COM module. Hence, all the modules are accessed using one application. The application has a Graphical User Interface (GUI) which is used for passing parameters to the program. The images from the CCD camera are written in FITS (Flexible Image Transport System) format as three-dimensional data cubes and are visualised using ActiveX component of Interactive Data Language (IDL) data analysis software. A snapshot of the data acquisition and control software is given in Fig. 3.

### 3. Preliminary results

The first-light Stokes images of a sunspot from the instrument are shown in Fig. 4. These images show the Stokes signal in blue wing of the Fe I 630.2 nm line. Such

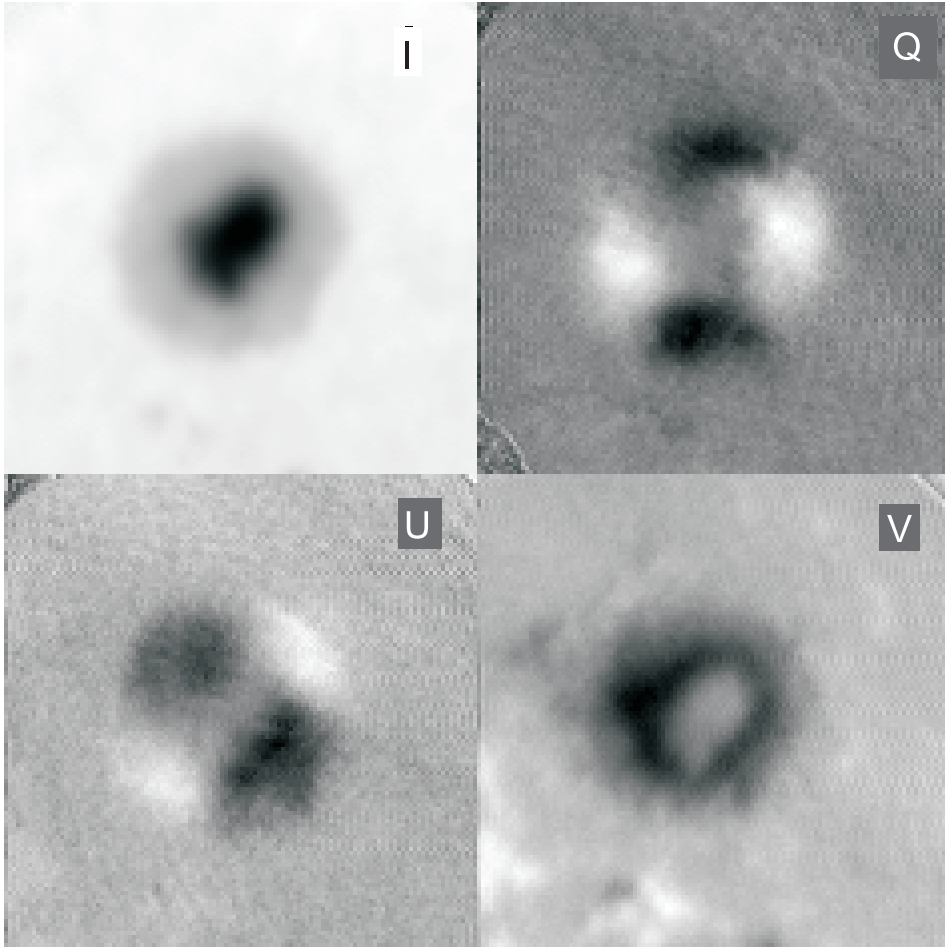


**Figure 4.** The first light observations represented here as Stokes I, Q, U and V images of a sunspot on the disk center. These images are obtained in the blue wing of Fe I 6302 line.

images are recorded all along the spectral line at discrete wavelength steps, the images are stacked to form a data-cube. The data-cube stores the Stokes profiles at all observed locations in the field-of-view. The data observed in this way is nearly free from seeing induced spurious polarization as these images are observed simultaneously. In principle the magnetic field vector can be deduced using the polarized images at only one wavelength position. This method relies on the calibration model to convert measured polarization to magnetic field. With measurements at only one wavelength position there are ambiguities, which are removed by measuring polarization at two or more wavelength positions in blue and red wings of the line (Hagyard & Kineke 1995). This method has been used successfully at various observatories around the world (Hagyard *et al.* 1982; Wang *et al.* 1998; Zhang H 2000; Sakurai *et al.* 1995) and is very suitable for studying magnetic field evolution in relation to solar flares. However, it is generally accepted that more accurate vector magnetic fields are derived by measuring full polarization spectral profiles. In this case, the observed profiles are inverted by

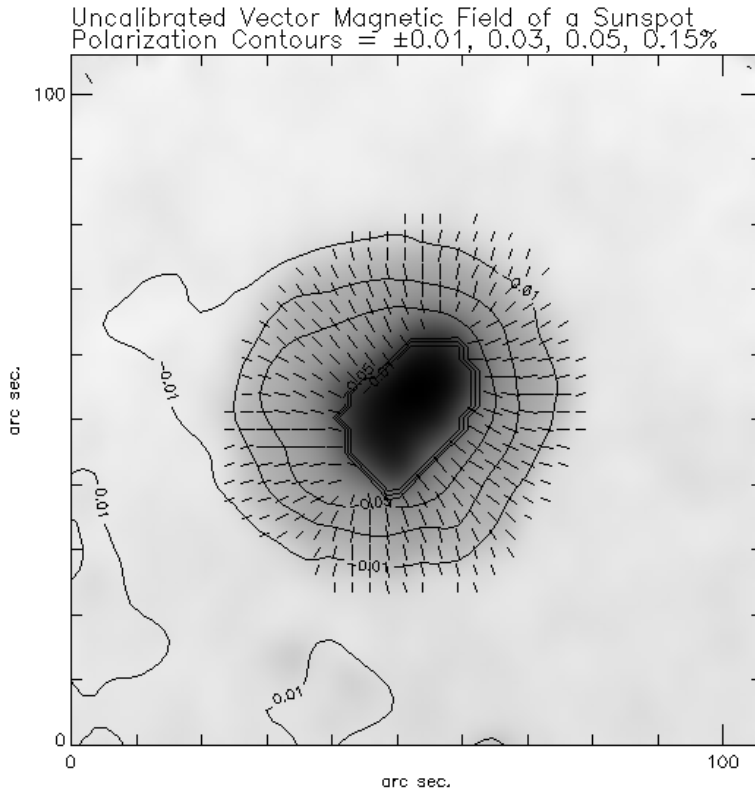


**Figure 5.** The uncalibrated vector magnetic field maps of a sunspot are shown using Stokes images of Fig. 4. The contours show the circular polarization degree, which is representative of line-of-sight magnetic field strength. The direction of the arrows represent the direction of transverse vector field.

non-linear least-squares fitting procedures, where a model atmosphere which yields observed profiles is searched. This approach is planned to be followed for the analysis of the SVM-I observations. Here, in a very preliminary analysis we present the uncalibrated vector field map in Fig. 5. The purpose is to check transverse field directions for their consistency with the configuration typically seen in sunspots. The observations are being further analyzed currently in order to determine the accuracies and sensitivity of the measurements, which will be published in a separate paper.

### Acknowledgements

We acknowledge help from the technical staff at Udaipur Solar Observatory in particular Mr. B. L. Paneri who developed the mechanical mounts for the optics and Mr. Sudhir Gupta who helped in developing the telescope tracker drive. Also, we acknowledge help from Computer Science Department of Mohanlal Sukhadia University, Udaipur for providing student trainees who helped in SVM-I software development.

**References**

- Choudhary Debi Prasad, Sanjay Gosain 2002, *Experimental Astronomy*, **13**, 153.
- Hagyard, M. J., Cumings, N. P., West, E. A., Smith, J. E. 1982, *Solar Phys.*, **80**, 33.
- Hagyard, M. J., Kineke, J. I. 1995, *Solar Phys.*, **158**, 11.
- Hicks, T. R., Reay, N. K., Atherton, P. D. 1984, *J. Phys. E: Sci. Instrum.*, **17**, 49.
- Sakurai, T., Ichimoto, K., Nishino, Y., Shinoda, K., Noguchi, M., Hiei, E., Li, T., He, F., Mao, W., Lu, H., Ai, G., Zhao, Z., Kawakami, S., Chae, J. 1995, *PASJ*, **47**, 81.
- Sankarasubramanian, K., Venkatakrishnan, P. 1998, *Optics & Laser Technology*, **30(1)**, 15.
- Wang, H., Denker, C., Spirock, T., Goode, P. R., Yang, S., Marquette, W., Varsik, J., Fear, R. J., Nenow, J., Dingley, D. D. 1998, *Solar Phys.*, **183**, 1.
- Zhang, H. 2000, *Solar Phys.*, **197**, 235.